



Middle Jurassic tracks of sauropod dinosaurs in a deep karst cave in France

Jean-David Moreau, Vincent Trincal, Emmanuel Fara, Louis Baret, Alain Jacquet, Claude Barbini, Remi Flament, Michel Wienin, Benjamin Bourel & Amandine Jean

To cite this article: Jean-David Moreau, Vincent Trincal, Emmanuel Fara, Louis Baret, Alain Jacquet, Claude Barbini, Remi Flament, Michel Wienin, Benjamin Bourel & Amandine Jean (2020): Middle Jurassic tracks of sauropod dinosaurs in a deep karst cave in France, *Journal of Vertebrate Paleontology*, DOI: [10.1080/02724634.2019.1728286](https://doi.org/10.1080/02724634.2019.1728286)

To link to this article: <https://doi.org/10.1080/02724634.2019.1728286>



[View supplementary material](#)



Published online: 25 Mar 2020.



[Submit your article to this journal](#)



[View related articles](#)



[View Crossmark data](#)



ARTICLE

MIDDLE JURASSIC TRACKS OF SAUROPOD DINOSAURS IN A DEEP KARST CAVE IN FRANCE

JEAN-DAVID MOREAU^{*,1}, VINCENT TRINCAL^{2,3}, EMMANUEL FARA¹, LOUIS BARET⁴, ALAIN JACQUET⁴, CLAUDE BARBINI⁴, REMI FLAMENT⁵, MICHEL WIENIN⁶, BENJAMIN BOUREL⁷, and AMANDINE JEAN⁷

¹CNRS UMR 6282 Biogéosciences, Université de Bourgogne Franche-Comté, 6 boulevard Gabriel, 21000 Dijon, France, jean.david.moreau@gmail.com; emanuel.fara@u-bourgogne.fr;

²Laboratoire Matériaux et Durabilité des Constructions, Institut National des Sciences Appliquées/Université Toulouse III-Paul Sabatier, 135 avenue de Rangueil, 31077 Toulouse, France;

³Département Génie Civil et Environnemental, Ecole des Mines, Institut Mines Télécom Lille Douai, Université de Lille, 764, boulevard Lahure, 59508 Douai, France, vincenttrincal@gmail.com;

⁴Association Paléontologique des Hauts Plateaux du Languedoc, 14 chemin des Ecureuils, 48000 Mende, France, louisbaret@netc.fr; alainjacquet48@hotmail.com; barbini.claude@sfr.fr;

⁵SARL Jardin des Arts, 12 rue Pannessac, 43000 Le Puy-en Velay, France, verticavite@gmail.com;

⁶Parc National des Cévennes, Place du Palais, 48400 Florac, France, michel@wienin.com;

⁷L'Université d'Aix-Marseille, CNRS, IRD, INRA, Collège de France, CEREGE, Aix-en-Provence, France, bourel@cerege.fr; jean@cerege.fr

ABSTRACT—Although the deep galleries of natural underground cavities are difficult to access and are sometimes dangerous, they have the potential to preserve trace fossils. Here, we report on the first occurrence of sauropod dinosaur tracks inside a karstic cave. Three trackways are preserved on the roof of the Castelbouc cave 500 m under the surface of the Causse Méjean plateau, southern France. The tracks are Bathonian in age (ca. 168–166 Ma), a crucial but still poorly known time interval in sauropod evolution. The three trackways yield sauropod tracks that are up to 1.25 m long and are therefore amongst the largest known dinosaur footprints worldwide. The trackmakers are hypothesized to be titanosauriforms. Some of the tracks are extremely well preserved and show impressions of digits, digital pads, and claws. We erect the new ichnogenus and ichnospecies *Occitanopodus gandi*, igen. et isp. nov. In order to characterize depositional environments, we conducted sedimentological, petrographic, and mineralogical analyses. The tracks from Castelbouc attest the presence of sauropods in proximal littoral environments during the Middle Jurassic. This discovery demonstrates the great potential of prospecting in deep karst caves that can occasionally offer larger and better-preserved surfaces than outdoor outcrops.

SUPPLEMENTAL DATA—Supplemental materials are available for this article for free at www.tandfonline.com/UJVP

Citation for this article: Moreau, J.-D., V. Trincal, E. Fara, L. Baret, A. Jacquet, C. Barbini, R. Flament, M. Wienin, B. Bourel, and A. Jean. 2020. Middle Jurassic tracks of sauropod dinosaurs in a deep karst cave in France. Journal of Vertebrate Paleontology. DOI: 10.1080/02724634.2019.1728286.

INTRODUCTION

The Middle Jurassic was a crucial period in sauropod evolution because it corresponds to the interval just preceding the Late Jurassic large radiation of Neosauropoda (Upchurch and Martin, 2003; Mannion et al., 2019). However, bones of Middle Jurassic sauropods are extremely sparse throughout the world (Weishampel et al., 2004; Mannion et al., 2019). In this context, tracksites are precious evidence to reconstruct the evolution of this dinosaur group during this important time period.

Although sauropod tracks are relatively common in the Lower and Upper Jurassic of Europe, they remain extremely rare in Middle Jurassic deposits. Occurrences have been reported from Aalenian–Bathonian tracksites in Denmark (Milà and Bromley, 2005; Milà, 2011), Portugal (Santos et al., 1994, 2009), Scotland (Brusatte et al., 2015), and the United Kingdom

(Romano et al., 1999; Day et al., 2002, 2004). In France, the putative Middle Jurassic sauropod tracks described by Sciau et al. (2006) have been reinterpreted as erosion structures and traces of trunks by Gand et al. (2007, 2018). Thus, definitive Middle Jurassic sauropod tracks have hitherto been unknown in France, whereas rare theropod trackways are reported from this geological interval (Sciau et al., 2006; Moreau et al., 2012; Moreau, 2017; Gand et al., 2018).

Here, we report on Middle Jurassic sauropod trackways that were discovered during speleological prospecting in the Castelbouc karstic network (Causses Basin, southern France) (Figs. 1, 2). Although dinosaur tracksites inside anthropic cavities (e.g., underground quarries or mines, railway tunnels) are well known around the world (e.g., Peterson, 1924; Parker and Balsley, 1989; Ahlberg and Siversen, 1991; Lockley and Hunt, 1995; Belvedere et al., 2008; Cook et al., 2010), the discovery of dinosaur tracks inside a natural karstic cave is extremely rare (e.g., theropod tracks from the Hettangian deposits of the Bramabiau and Malaval caves in southern France; Ellenberger, 1988; Moreau et al., 2018). The trackways from Castelbouc represent the first occurrence of sauropod tracks inside a natural karstic cave.

*Corresponding author.

Color versions of one or more of the figures in the article can be found online at www.tandfonline.com/ujvp.



FIGURE 1. The Tunnel gallery in the Castelbouc No. 4 Cave, view from the east. Photograph by Rémi Flament.

HISTORICAL AND GEOLOGICAL CONTEXT OF THE CAVE

The Castelbouc karstic network is located in the northern part of the Causses Basin, 500 m under the surface of the Causse Méjean plateau, Lozère Department (Fig. 2A). Entrances to the network are located in the Gorges du Tarn, 30 km south of Mende (André, 1992). The Castelbouc caves have probably been known since pre-Medieval times (André, 1992). They are well known locally for flooding after rainy events. They consist of two large caves (Castelbouc caves No. 1 and No. 4) and two karst springs (Castelbouc caves No. 2 and No. 3). The dinosaur tracks presented here are located in cave No. 4. In 1952, the known part of the Castelbouc No. 4 cavity was limited to a first gallery called the ‘Sous-Préfet’ gallery (Fig. 2A). After many excavations since 1952, this cave is now 880 m long and exhibits 102 m of difference in elevation (André, 1992). The first dinosaur tracks were discovered by one of us (J.-D.M.) in 2015 during a speleological trip. Three scientific missions were organized in 2016, 2017, and 2018. Tracks are located on the roof of the Tunnel gallery (Fig. 2). This large gallery is 76 m long, up to 22 m wide, and up to 11.5 m high. The access to the Tunnel gallery is only possible by crawling along very narrow labyrinthine conduits about 100 m long. Because some portions of these small conduits periodically flood, access to the far galleries requires caution and is limited to drought periods.

The Castelbouc No. 4 cave occurs in the ‘Calcaires à stipites’ Formation, which is between 30 and 150 m thick in this area (Charcosset et al., 1996; Ciszak et al., 1999). It consists of gray limestone alternating with thin layers of lignitic marl, and white

oolithic limestone. Regionally, in the southern part of the Causses Basin, lenticular lignitic beds of the ‘Calcaires à stipites’ Formation were mined for coal (Rouire, 1946). Based on ammonites, brachiopods, and foraminiferans, this formation is considered to be lower to upper Bathonian in age (Charcosset, 2000; Gand et al., 2018, and references therein).

METHODS

In order to characterize depositional environments, sedimentological, petrographic, and mineralogical analyses were conducted along a 9-m-thick stratigraphic section accessible in the Tunnel gallery. Nine samples were prepared on standard polished thin sections for both optical microscopy (with a Zeiss Axiozoom macroscope) and mineralogical analyses.

X-ray Diffraction (XRD) Mineralogy

Powders (thoroughly dried and micronized by grinding in an agate mortar and pestle) were analyzed using a Bruker D8 Advance diffractometer system using Co-K α radiation equipped with a fast LynxEye position sensitive detector (wave length [WL] = 1.78897). The diffractometer was operated at 35 kV and 40 mA. Scans were run from $2\theta = 5^\circ$ to $2\theta = 80^\circ$, with a step interval of $2\theta = 0.02^\circ$ and a time acquisition of 96 s per step. The identification of minerals was performed using Bruker AXS DiffracPlus EVA software and the ICDD (the International Centre for Diffraction Data) Powder Diffraction File 2015 database.

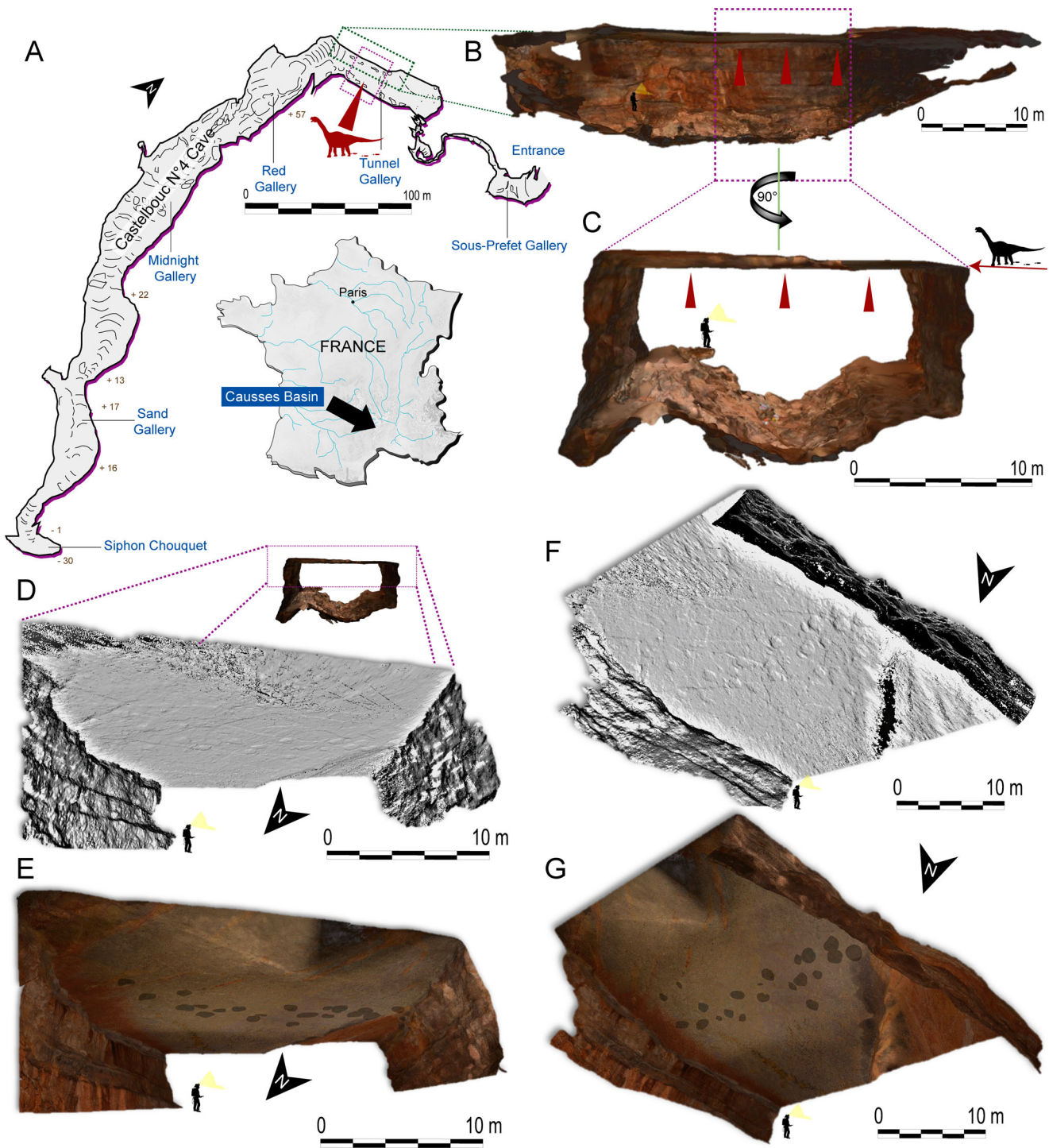


FIGURE 2. Castelbouc No. 4 Cave and details of the gallery yielding dinosaur tracks. **A**, location of the Causses Basin in France and topography of the cave showing the location of the Tunnel gallery. **B, C**, photogrammetric 3D textured meshes of the part of the gallery yielding ichnofossils, in **B**, longitudinal east–west section and **C**, transversal north–south section; red arrows indicate the surface bearing traces. **D–G**, photogrammetric 3D meshes of the roof of the gallery yielding tracks in two different views: **E, G**, with and **D, F**, without texture.

Mineral quantification of the rock samples was made by Rietveld analysis (e.g., Bish and Post, 1993) with the DIFFRACplus TOPAS software, version 4.2 (Bruker AXS). The Rietveld method consists of minimizing the difference between an experimental diffractogram and a diffractogram calculated for a given starting model. Crystal structure data were taken from the

ICDD PDF and Bruker Structure Database. Rietveld refined parameters used in this study are the same as described in Tricnal et al. (2014). Standard deviations of mineral contents were obtained by the multiplication of the standard deviation given by Topas software by the GOF (goodness of fit) in order to provide a more realistic approximation of error (Taylor and

Hinczak, 2003; Trincal et al., 2014). However, it must be kept in mind that this method does not evaluate amorphous phases but only well-crystallized ones detected by XRD.

The percentage of amorphous versus crystallized minerals was estimated by the simple qualitative method as provided in the Bruker EVA software using the following equations (1 and 2):

$$\% \text{Amorphous} = \frac{\text{Global area} - \text{Reduced area}}{\text{Global area}} \times 100 \quad (1)$$

$$\% \text{Crystallinity} = 100 - \% \text{Amorphous} \quad (2)$$

where the global area includes all peaks and the ‘hump’ due to any X-ray amorphous material and the reduced area is the background-subtracted scan, the subtraction including the amorphous ‘hump.’

Carbonate Quantification

Thermogravimetry coupled with mass spectrometry (TGA-MS) analyses were conducted using a Netzsch STA449F3 Jupiter thermal analyzer coupled with a Netzsch QMS403D Aëlos quadrupole mass spectrometer. Setup was configured for a temperature increase of 3°C/minute from 100°C to 1,000°C under an argon stream. This method, well adapted for sedimentary rocks (e.g., Moreau et al., 2018), measures quantitative mass loss and qualitative gas production generated by carbonate calcination. Because it includes amorphous phases, this method is complementary to the Rietveld quantifications.

X-ray Fluorescence (XRF) Chemistry

Bulk-rock chemical analyses were performed using a Bruker S4 Pioneer spectrometer, a 4 kW wavelength dispersive X-ray fluorescence spectrometer equipped with a rhodium anode. Measurements were performed at 60 keV and 40 mA on powdered-rock compressed tablets. The integrated standardless evaluation of the machine provides a fast and easy semiquantitative determination of element concentrations down to the ppm level without performing a calibration. Carbon was detected but not quantified with this method. XRF analyses were used for modal calculation following the method used in Trincal et al. (2014). This method consists in distributing all the chemical elements in the identified mineral phases and in quantifying them. As for ATG-MS, these estimates include the amorphous content of the rock (excluding organic matter) and could differ from results obtained by the Rietveld method. This method is used to qualitatively cross-validate previous results. Optical microscopy, X-ray fluorescence (XRF) spectrometry, X-ray diffraction (XRD), and loss on ignition measures (on only one sample) were performed at the Department of Civil and Environmental Engineering of Institut Mines Télécom Lille Douai (Trincal et al., 2018).

Trace Fossil Analysis

The descriptive terminology and biometric parameters used in this study follow Marty (2008). We used the following standard abbreviations (Fig. S1, Supplemental Data): **a**, pedal track rotation; **b**, manual track rotation; γ , pedal track pace angulation; δ , manual track pace angulation; **Dm-p**, manual track–pedal track distance; **iTW**, inner trackway width; **LMP**, left manual track pace length; **LPP**, left pedal track pace length; **ML**, manual track length; **MS**, manual track stride length; **mSW**, manual track side width; **MW**, manual track width; **oTW**, outer trackway width; **PL**, pedal track length; **PS**, pedal track stride length; **pSW**, pedal track side width; **PW**, pedal track width; **RMP**, right manual track pace length; **RPP**, right pedal track pace length; **WAM**, width of the manual

track angulation pattern or manual trackway width; and **WAP**, width of the pedal track angulation pattern or pedal trackway width. The glenoacetabular distance (GA), which corresponds to the distance between the center of the shoulder joint (glenoid cavity) and the center of the hip joint (acetabular cavity) was estimated by measuring the distance between the midpoint of a line connecting two consecutive pedal tracks (left and right or vice versa) and the midpoint of a line connecting the next two manual tracks (Fig. S1). Parameters were measured on the roof of the cave using a Leica DISTO X310 laser distance meter (precision of ± 1 mm) combined with a Bosch Quigo Cross line laser. Measured values are listed in Table 2.

In addition to the parameters measured directly on tracks and trackways, several parameters were calculated. Following Thulborn (1990), index of pedal track size (IPS) was calculated using the formula $(PL \times PW)^{0.5}$, and index of manual track size (IMS) was calculated using the formula $(ML \times MW)^{0.5}$. Heteropody consists of the difference in area (total track area) between the pedal and manual tracks. The area of each track was calculated using the software ImageJ (version 1.43u; Schneider et al., 2012). According to Marty (2008), the trackway gauge was estimated using the pedal trackway ratio (PTR) as given in Equation 3:

$$\text{PTR} = \frac{\text{Side width(SW)}}{\text{Overall width(OW)}} \times 100\% \quad (3)$$

with wide gauge $< 40\%$ $<$ medium gauge $< 50\%$ $<$ narrow gauge, and the WAP/PL ratio, with narrow gauge $< 1.0 <$ medium gauge $< 1.2 <$ wide gauge.

Based on Alexander’s (1976) formula (Equation 4), the locomotion speed (v) was estimated using the calculated hip height (h) and the measured value of stride length (S) as follows:

$$v = 0.25g^{0.5} \times S^{1.67} \times h^{-1.17} \quad (4)$$

As explained by Salisbury et al. (2017), the glenoacetabular length typically exceeds the osteological hip height in early sauropodomorphs, and although these two lengths converge in later sauropods (Paul, 2010), the hip height rarely exceeds the glenoacetabular distance. Following Salisbury et al. (2017), the hip height was estimated using the length of the glenoacetabular distance.

Photogrammetry

In order to produce photogrammetric three-dimensional (3D) reconstructions of the gallery and orthoimages of the track-bearing surface, the software Agisoft PhotoScan Professional 1.2.4 was used to align and combine multiple digital photographs taken by a Nikon D5200 camera coupled with an AF-S NIKKOR 18–105 mm f/3.5–5.6G ED camera lens. The same software was used to produce photogrammetric 3D textured meshes. Shadows were applied on 3D reconstructions using the MeshLab 1.3.2 software (Cignoni et al., 2008). The 3D meshes are available online at <https://figshare.com>.

RESULTS

Stratigraphy and Petrography

The stratigraphic column exposed in the Tunnel gallery displays limestone beds alternating with fossiliferous lenticular clayey layers (Fig. 3). Three lignitic lenses and three main erosive surfaces have been identified (S1–S3). We distinguish seven facies, F1 to F7 (see Table 1 and Figs. 3, 4). F1 consists of gray marl yielding fossil plants such as leafy axes of conifers. F2 is a gray to blue cryptalgal limestone showing abundant thin

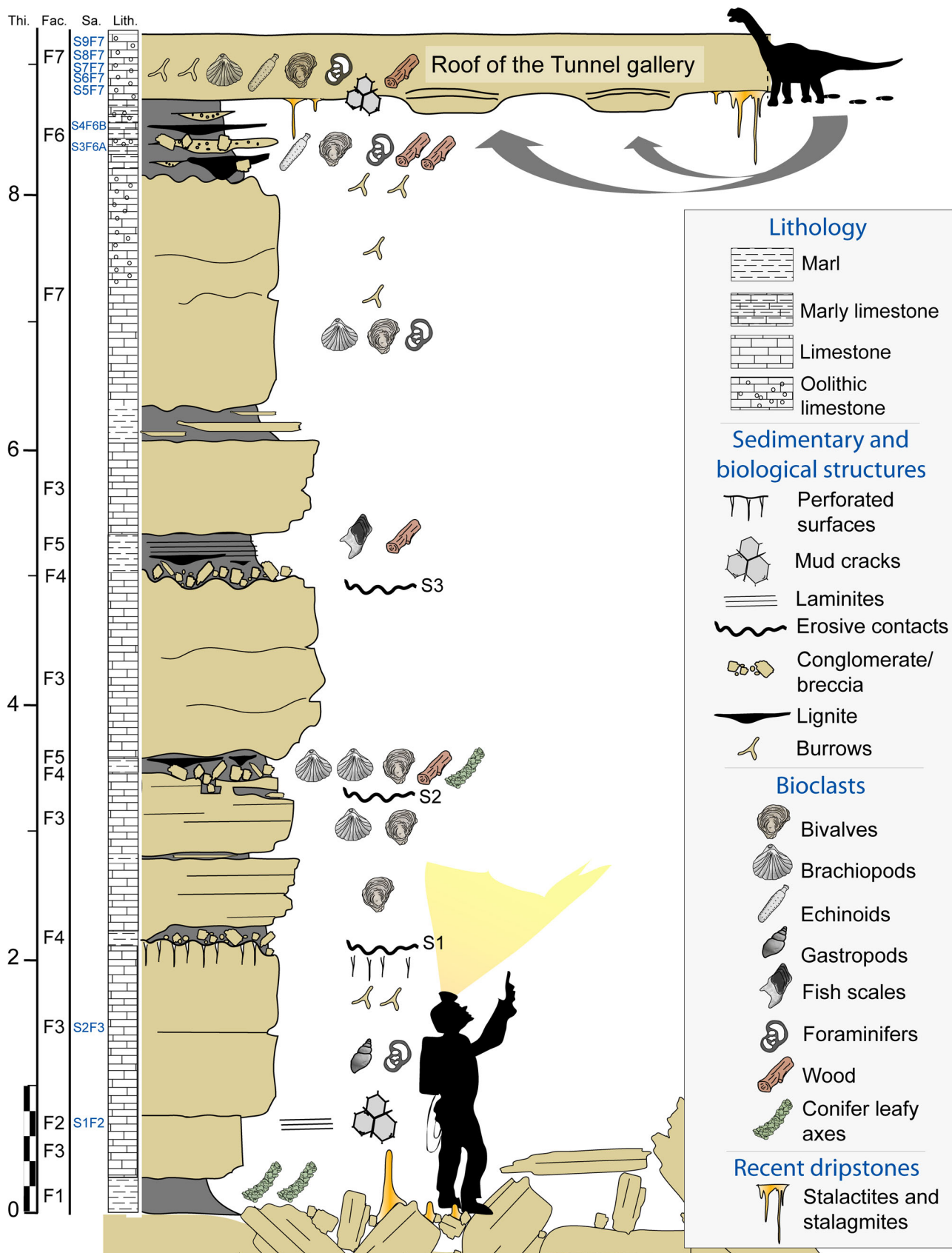


FIGURE 3. Stratigraphic section of the Tunnel gallery showing location of dinosaur tracks. Abbreviations: **Fac.**, facies; **Lith.**, lithology; **Sa.**, location of samplings; **Thi.**, thickness (m).

TABLE 1. Microfacies.

No.	Facies	Textures	Description	Depositional environments
F1	Gray marl	M	Gray marl. Some leafy axes of conifers (compressions with cuticle) ascribed to <i>Brachiphyllum</i> sp. and <i>Pagiophyllum</i> sp.	Shallow environment not open to the sea (backshore?).
F2	Cryptalgal laminites	M (P)	Gray/blue limestone with abundant thin laminites. No bioclasts. Mud cracks. Microbial mats. Microbial laminae parallel to the bedding planes and wavy to planar. Nonporous fabric.	Intertidal to supratidal zone. Tidal flat. Periodic emersions.
F3	Bioclastic limestone	M-W(P)	Gray/blue bioclastic limestone (pelbiomicrite). Abundant peloids, some ooids. Bioclasts including bivalves, brachiopods, corals, foraminiferans, and gastropods. Burrows.	Shallow environment not far from the shore.
F4	Lignitic breccia	P	Coaly breccia with angular/subangular limestone blocs in green/brown/black clayey matrix.	Foreshore/beach. High hydrodynamism.
F5	Bioclastic marl	W(P)	Gray marl with thin layer of lignite yielding micro- and macroremains of wood. Bivalves, brachiopods. Rares <i>Lepidotes</i> scales.	Low-energy coastal environment, such as lagoon or enclosed bay.
F6	Lignitic oncoidic to peloidal marly limestone	M-W-P	Gray/blue or black marly limestone locally bearing centimetric to decimetric lignitic oncoidic to peloidal lenses with short lateral extensions. Abundant compressed woods, as wells as fragments of bivalve shells, corals, foraminiferans, and spines of urchins. Intraclasts of oomicrite limestone.	Border of a shallow, restricted environment (bay or lagoon), periodically emerged or open to the sea. Brackish?
F7	Oolithic limestone	P(W)	Gray oopelmicrite and peloomicrite locally with abundant fragments of bivalves, brachiopods, corals, benthic foraminiferans (miliolids), and echinoids. Some microremains of wood.	Shoreface to foreshore. High energy shoals.

Abbreviations: **M**, mudstone; **P**, packstone; **W**, wackestone.

laminites with mud cracks and microbial mats (Fig. 4A). F3 consists of gray to blue limestone (a pelbiomicrite) with marine bioclasts (Fig. 4B). F4 is a green, brown to black marly and coaly breccia. F4 corresponds to the facies overlying erosion surfaces S1–S3. F5 consists of lignitic and bioclastic marl yielding abundant marine remains. F6 is a gray/blue marly limestone (facies F6 type A [F6A]; Fig. 4C) locally bearing centimetric to decimetric black lignitic and oolithic, oncoidic to peloidal lenses yielding abundant intraclasts and bioclasts (bivalve shells, corals, foraminiferans, and spines of sea urchins) (facies F6 type B [F6B]) with short lateral extensions (Fig. 4D, E). F7 consists of gray oolithic limestone (oopelmicrite to peloomicrite) with abundant marine bioclasts as well as rare wood microremains (Fig. 4F).

Mineralogy

Rietveld mineralogical quantifications indicate that the crystallized fraction is very homogenous, with more than 92 weight% (wt%) of calcite, less than 5 wt% of illite/muscovite, less than 2 wt% of quartz and dolomite, and less than 1 wt% of rutile (Figs. S2–S4; Tables S1–S3). The sample S3F6A (marly limestone) is distinguished by 82 wt% of calcite and 15 wt% of illite/muscovite, but this difference is not found laterally in S4F6B (lignitic marly limestone). Gypsum was identified only in sample S4F6B, with almost 1 wt%. The percentage of crystallinity ranges from 80 to 88 wt% in all samples. The remaining 12–20 wt% can be attributed to organic matter and/or to poorly crystallized minerals. Organic matter was detected by XRF in all samples and observed on thin section mainly in the sample S4F6B (Fig. 4). Its content was quantified at 2.25 wt% by loss on ignition in sample S4F6B. The ratio of crystallinity to illite/muscovite content suggests that the more phyllosilicates there are, the higher the ‘amorphous’ content. Modal calculations performed with XRF data as well as calcite quantification by TGA-MS (Figs. S3, S4; Tables S2–S4) suggest that calcite is slightly overvalued at the expense of other minerals, especially in clayed facies. All these elements

are consistent with the hypothesis that the amorphous fraction is enriched with small and poorly crystallized illite/muscovite at the expense of carbonates.

Tracks and Their Preservation

The roof of the Tunnel gallery bears three trackways of sauropods (Castelbouc 1, CAS-1; Castelbouc 2, CAS-2; and Castelbouc 3, CAS-3; Figs. 5–8). This surface is located at a height of 7.9–10.9 m above the floor of the cavern. We distinguish two trackway morphologies: quadrupedal, wide-gauge trackways (CAS-1 and CAS-2) and pedal-track-only, narrow-gauge trackways (CAS-3). All of them can be classified as large sauropod trackways (pedal track length ca. 75 cm) according to the size classes proposed by Marty (2008).

The tracks occur at the interface of a marly limestone bed locally showing lignite lenses (facies F6; Fig. 3) and a peloomicrite bed containing abundant marine organisms (F7). Due to erosion of the marly limestone, concave epireliefs are not preserved. Only the infilled convex hyporeliefs are preserved on the roof of the cave (facies F7; Fig. 3).

The preservation of tracks is variable among the three trackways. Trackway CAS-1 shows well-preserved pedal and manual tracks. The outlines of the tracks composing CAS-2 are weakly marked and not complete. Several parameters cannot be definitively measured on this trackway (Table 2). The pedal-track-only trackway CAS-3 shows exquisite details of claws and pads.

SYSTEMATIC PALEOICHNOLOGY *OCCITANOPODUS GANDI*, igen. et isp. nov. (Figs. 5, 6; Fig. S5)

Holotype—Manual track-pedal track set LM1-LP1 of the trackway CAS-1 preserved in situ on the roof of the Castelbouc No. 4 Cave (Lozère, southern France).

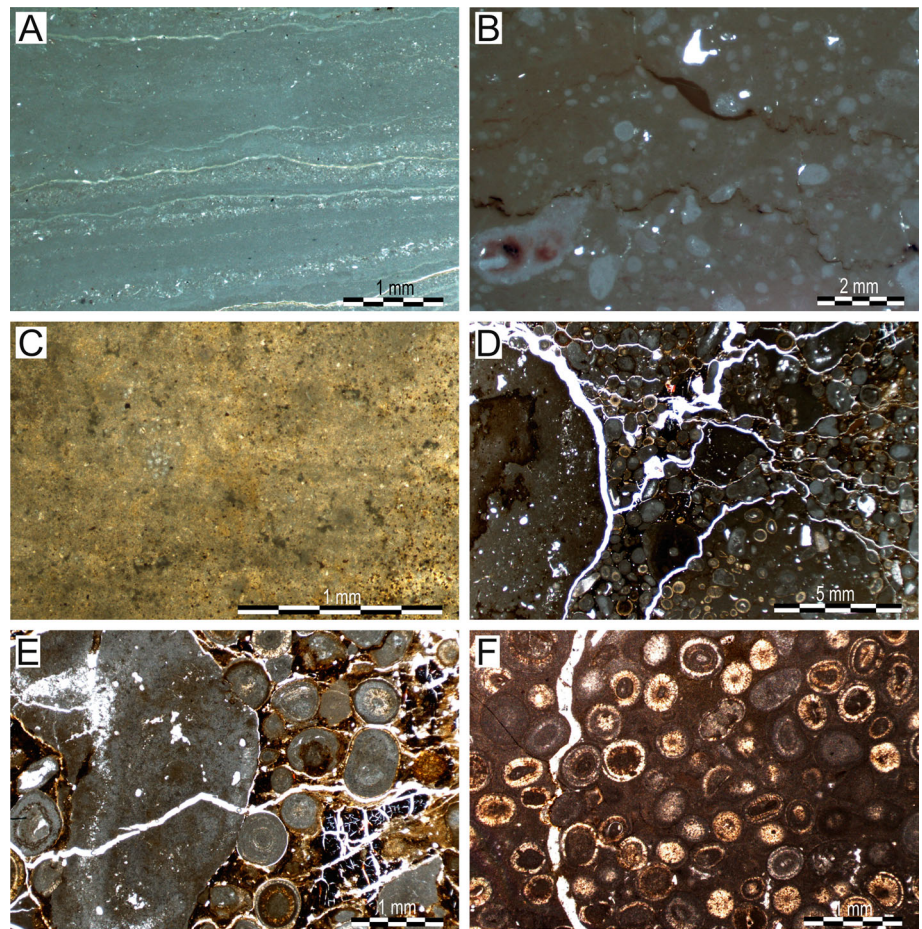


FIGURE 4. Microfacies F2–F6. **A**, cryptalgal laminites with micrite and sparite layers (F2). **B**, pelbiomicrite showing stylolites (F3). **C**, marly limestone (F6A). **D**, **E**, lignitic marly limestone showing ooliths, oncoids, and peloids (F6B). **F**, oopelmicrite (F7).

Locality, Horizon, and Age—The tracksite occurs in the Tunnel gallery of the Castelbouc No. 4 Cave. Middle Jurassic, Bathonian, ‘Calcaires à Stipites’ Formation.

Diagnosis—Ichnotaxon showing a unique combination of characters not observed amongst other wide-gauge sauropod tracks such as *Brontopodus*, *Polyonyx*, and *Titanopodus*, as well as medium- to wide-gauge sauropod tracks such as *Calorckosauripus* and *Oobardjidama*. Trackway: wide-gauge sauropod trackway with pronounced heteropody (pedal track area 4–6 times greater than manual track area). Pedal tracks and manual tracks aligned. Pedal tracks: form a small positive rotation angle relative to the trackway axis (0–27°). Large-sized (about 1 m in length), pentadactyl, asymmetric, subcircular to oval pedal tracks. Pedal tracks mainly as long as wide or slightly wider than long. Maximum width of pedal tracks located in the middle, or slightly toward the anterior part of the track. Pedal tracks with short digit impressions that show strong outward rotation. Manual tracks: form a small positive rotation angle relative to the trackway axis (0–27°). Manual tracks symmetrical, ‘D’-shaped, and lacking any indication of digits or claws.

Etymology—The ichnogenus is derived from the ‘Occitanie’ region and Greek ‘podus’ for foot. The ichnospecies is dedicated to French paleoichnologist Prof. Georges Gand.

Description—Trackway CAS-1 is straight, about 18 m long, 2.6 m wide, and includes 12 pedal tracks and 10 manual tracks (at least five strides; Fig. 5, 7). Because the WAP/PL ratio is between 1.2 and 2 and the PTR value is 39%, the trackway CAS-1 can be considered wide-gauge. The pedal tracks and the

manual tracks are aligned on both sides of the midline trackway. Pedal track and manual track stride lengths are 3.2–3.5 and 3.1–3.5 m, respectively. Pedal track and manual track paces are very similar, both being 2.0–2.3 m long. Heteropody is pronounced though not constant along the trackway (1:4–1:6). Most of pedal tracks show a small positive rotation angle relative to the trackway axis ($\alpha = 0–27^\circ$). The pedal tracks are asymmetric, subcircular to oval in shape, and pentadactyl (Fig. 6). Pedal tracks are mainly as long as wide, with variable length and width within and between trackways. Pedal tracks are 56–94 cm long and 82–116 cm wide (IPS = 77–100). In most pedal tracks, the maximum width is located in the middle, or slightly toward the anterior part of the track. Traces of digits are very short and are strongly rotated outward. Most of manual prints show a small positive rotation angle with the trackway axis ($\beta = 0–27^\circ$). Outlines of manual tracks are well marked and do not seem to be deformed by the pedal tracks. The manual prints are symmetric, ‘D’-shaped, and always convex forward. They are wider than long. They are 21–47 cm long and 40–76 cm wide (IMS = 33–53). Digit impressions are not marked.

Remarks—The PTR value suggests that CAS-1 is not so far from the medium gauge category ($40\% < \text{PTR} < 50\%$) defined in Marty (2008). As seen in some manual track–pedal track sets (e.g., LM1-LP1), the manual track is clearly distinct from the pedal track, showing that the high heteropody values cannot be explained by the overlap of manual imprints by pedal tracks. The glenoacetabular distance of the trackmaker is estimated to be 2.3–2.7 m. We estimated the hip height of the trackmaker to be 2.5 m.

TABLE 2. Biometric data of sauropod trackways from Castelbouc.

Dimension	CAS-1		CAS-2		CAS-3	
	Average	Min-Max	Average	Min-Max	Average	Min-Max
Pedal track length (PL)	85	56–94	77	64–98	122	119–125
Pedal track width (PW)	102	82–116	103	96–109	100	99–102
Index of pedal track size (IPS)	92	77–100	89	83–104	111	110–112
Pedal track rotation (α)	14°	0–27°	—	—	38°	26–40°
Manual track length (ML)	34	21–47	27	23–31	—	—
Manual track width (MW)	62	40–76	65	49–81	—	—
Index of manual track size (IMS)	45	33–53	41	34–50	—	—
Manual track rotation (β)	14°	0–27°	—	—	—	—
Trackway orientation	N290°	—	N130°	—	N125°	—
Pedal track stride length (PS)	334	320–346	341	325–357	440	—
Width of the pedal track angulation pattern (WAP)	128	116–141	—	—	100	—
Right pedal track pace length (RPP)	206	197–222	—	—	239	—
Left pedal track length (LPP)	225	216–230	—	—	225	—
Pedal track pace angulation (γ)	104°	—	—	—	128°	—
Pedal track side width (pSW)	102	82–116	103	96–109	102	98–108
Manual track stride length (MS)	323	310–348	341	341	—	—
Width of the manual track angulation pattern (WAM)	134	112–160	—	—	—	—
Right manual track pace length (RMP)	218	203–232	—	—	—	—
Left manual track pace length (LMP)	216	206–221	—	—	—	—
Manual track pace angulation (δ)	100°	—	—	—	—	—
Manual track side width (mSW)	62	40–76	—	—	—	—
Outer trackway width (oTW)	—	260–270	—	—	210	—
Inner trackway width (itw)	—	30–40	—	—	—	—
Dm-p (manual track–pedal track distance)	77	55–105	60	52–68	—	—
WAP/PL	1.5	—	—	—	0.8	—
WAP/IPS	1.4	—	—	—	1.1	—
WAM/ML	3.9	—	—	—	—	—
WAP/IMS	2.8	—	—	—	—	—
Pedal trackway ratio (PTR)	39%	31–44%	—	—	49%	45–51%
Manual trackway ratio (MTR)	26%	22–30%	—	—	—	—
Glenoacetabular distance (GA)	249	230–270	—	—	—	—
Locomotion speed (v; km/h)	7.2	—	—	—	—	—

Linear measurements in cm.

UNDETERMINED SAUROPOD TRACKS

The Quadrupedal, Wide-Gauge Trackway CAS-2

Description—Trackway CAS-2 is about 15 m long and includes at least seven pedal tracks (two complete and five partial) and three manual tracks (Figs. 5, 7). The trackway is straight at its start and then is slightly curved to the right. Heteropody is pronounced (1:3–1:4). Pedal track and manual track stride lengths are 3.2–3.6 m. The pedal tracks are asymmetric, mainly oval, and wider than long. Pedal tracks are 65–98 cm long and 96–109 cm wide (IPS = 83–104). The manual prints are symmetric, crescent-shaped to ‘D’-shaped, and always convex forward. They are wider than long. They are 23–31 cm long and 79–81 cm wide (IMS = 34–50). Neither the manual tracks nor the pedal tracks show impressions of digits.

Remarks—Because the trackway is poorly preserved, we refrain from assigning CAS-2 to an ichnotaxon. CAS-2 differs from *Occitanopodus gandi*, igen. et isp. nov., in showing a lower heteropody.

The Pedal-Track-Only, Narrow-Gauge Trackway CAS-3

Description—Trackway CAS-3 is 5.2 m long, 2.1 m wide and includes three large pedal tracks (Fig. 8; Fig. S6). Manual tracks are absent. Based on a WAP/PL ratio of 0.8, as well as a PTR value up to 51%, the trackway can be considered to be a narrow-gauge trackway. Pedal track stride length is 4.4 m long. Pedal track pace is 2.25–2.39 m long. Pedal tracks show a pronounced positive rotation angle with the trackway axis (α = 26–40°). The pedal tracks are asymmetric, subtriangular in shape, longer than wide, pentadactyl, 119–125 cm long, and 99–102 cm

wide (IPS = 110–112). The maximum width of each pedal track is located toward the anterior part of the track. Pedal tracks exquisitely preserve impressions of digits and claws. Traces of digits are quite short, triangular in shape, longer than wide, and strongly rotated outward. Digits I and II are better marked than digits III and IV. Distally, digit I shows an oval pad impression (Fig. 8C; Fig. S6).

Remarks—Although manual tracks are not observed in CAS-3, narrow-gauge trackways with pedal tracks intersecting the trackway midline are characteristic of two Middle to Upper Jurassic sauropod tracks: *Breviparopus* Dutuit and Ouazzou, 1980, and *Parabrontopodus* Lockley et al., 1994. Whereas Wright (2005) suggested that *Parabrontopodus* may be a junior synonym of *Breviparopus*, Marty et al. (2010) considered both ichnotaxa valid. Although CAS-3 shares some similarities with *Breviparopus* (large pedal track length; large pedal track rotation up to 30°; pronounced heteropody; claw marks), it differs from this ichnogenus in showing a well-marked fifth digit. Because the manual tracks are missing, we refrain from assigning CAS-3 to an ichnotaxon.

DISCUSSION

Preservation of the Tracks

Pedal-track-only trackways similar to trackway CAS-3 are frequent in sauropod tracksites (e.g., Marty, 2008; Falkingham et al., 2011). It was sometimes explained by relatively small manual tracks being overprinted by subsequent, considerably larger pedal tracks (Marty, 2008). Alternatively, some sauropods may have been able to have an occasional bipedal stance over short distances (Wilson and Carrano, 1999). However, in most cases,

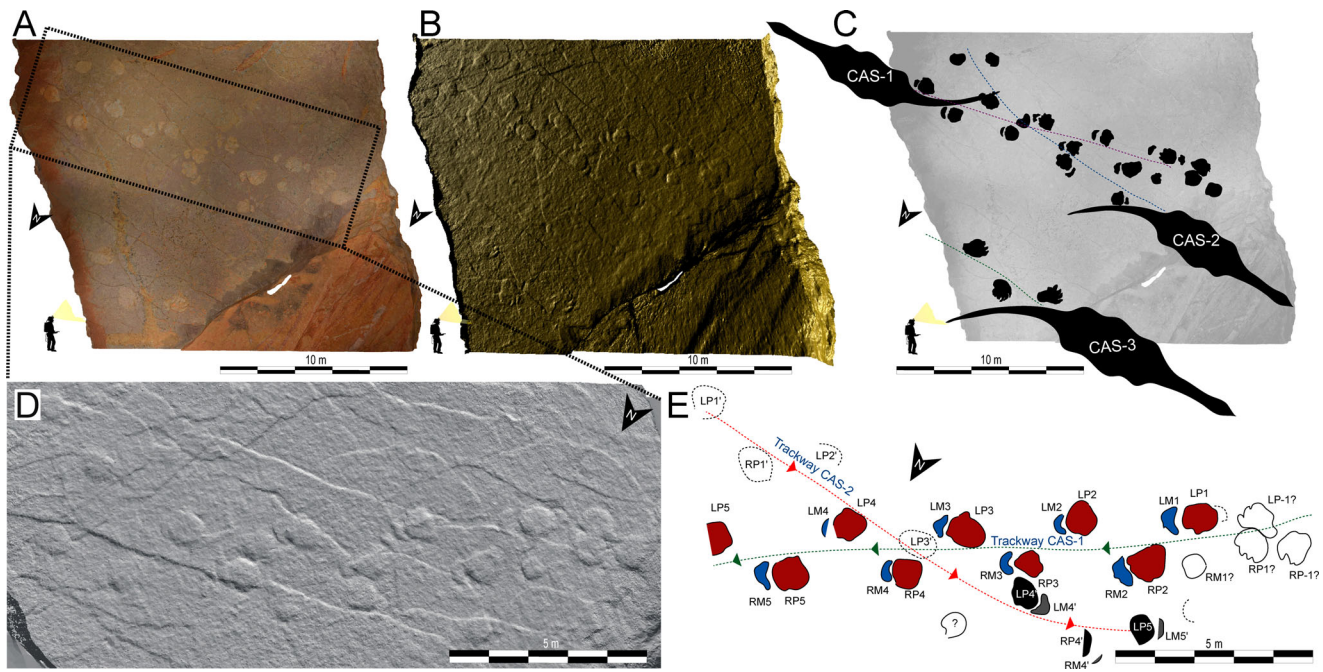


FIGURE 5. Surface of the roof of the Tunnel gallery bearing sauropod trackways. **A**, photogrammetric 3D textured mesh; **B**, photogrammetric 3D mesh (using the ‘dimple’ filter of the MeshLab software); **C**, interpretive sketch. **D**, **E**, detail of CAS-1 and CAS-2, showing **D**, a photogrammetric 3D mesh without texture and **E**, interpretive sketch.

the absence of manual tracks can be explained by preservational processes. When the foot does not penetrate the sediment but compresses it, it creates a stack of transmitted prints (‘stack of casts and moulds’ sensu Marty, 2008) called undertracks. They consist of more or less modified versions of the ‘true’ tracks depending of the vertical distance from the tracking surface (Marty, 2008). Because the pressures exerted by the manus and the pes were different (Falkingham et al., 2011), the deformation of the sediment is sometimes shallower below the tracked surface of the manus. It explains why some sauropod trackways only display pedal tracks. The presence of a pedal-track-only trackway, as well as the variable quality of preservation between CAS-1, CAS-2, and CAS-3, suggests multiple track-bearing surfaces on and above the roof of the cave. Because the tracks from Castelbouc are not visible in cross-section, we cannot confidently determine whether some of the tracks are actually ‘true’ tracks, undertracks, or natural moulds. If the walking surfaces are located above the roof of the cave, the exquisite details of claws and pads suggest that the ‘true’ walking surfaces were probably located very close to the roof.

Comparison of *Occitanopodus*, *igen. nov.*, with Other Tracks

Worldwide, Middle Jurassic sauropod trackways are ascribed to *Breviparopus* Dutuit and Ouazzou, 1980, *Brontopodus* Farlow et al., 1989, *Parabrontopodus* Lockley et al., 1994, and *Polyonyx* Santos et al., 1994. In Europe, although tracks remain unnamed in most Middle Jurassic tracksites, *Breviparopus*- and *Brontopodus*-like tracks were reported from the Aalenian of England (Yorkshire; Romano et al., 1999) and *Polyonyx gomesi* from the Bajocian–Bathonian of Portugal (Santos et al., 1994, 2009).

Breviparopus was erected based on Middle to Upper Jurassic trackways from Morocco (Dutuit and Ouazzou, 1980). This ichnogenus differs from *Occitanopodus* in showing narrow-gauge trackways with pedal tracks intersecting the trackway midline

(like CAS-3), manual tracks are located further away from the midline than pedal tracks, and it has a lower heteropody (i.e., 1:3).

Brontopodus was described based on material from the Lower Cretaceous of the U.S.A. (*B. birdi*; Farlow et al., 1989). *Brontopodus birdi* and *O. gandi*, *igen. et isp. nov.*, share some similarities, such as wide-gauge trackway, large size of pedal tracks (i.e., up to 100 cm), and clawless manual tracks. However, they are different for the following reasons. *Brontopodus birdi* differs in having pedal marks clearly longer than wide, as long as wide ‘U’-shaped manual prints that show rounded marks on digits I and V, and lower heteropody (i.e., 1:3 among *B. birdi*; Lockley et al., 1994). *Brontopodus pentadactylus* from the Lower Cretaceous of Korea clearly differs from *Occitanopodus* in having outwardly rotated manual prints and lower heteropody (i.e., 1:2; Kim and Lockley, 2012). *Brontopodus plagnensis* from the lower Tithonian of eastern France differs in showing a long, sharp anterolateral claw mark pointing posterolaterally on the impression of pedal digit V (Mazin et al., 2017).

Parabrontopodus was erected based on material from the Upper Jurassic of the U.S.A. (Lockley et al., 1994). In France, this ichnogenus was reported from the lower Kimmeridgian and the Tithonian from the Jura Department (Le Loeuff et al., 2006; Mazin et al., 2016). Although *Parabrontopodus* show medium- to large-sized tracks (i.e., 50–90 cm), strong heteropody (i.e., 1:4 or 1:5 in *P. mcintoshii*; Lockley et al., 1994), and manual tracks wider than long, this ichnogenus differs from *Occitanopodus* in showing narrow-gauge trackway characterized by the absence of space between the trackway midline and the inside margin of the pedal tracks. In addition, pedal tracks are longer than wide, with the long axis rotated outward.

Although *Polyonyx gomesi* consists of wide-gauge trackway with large pedal tracks (i.e., PL = 90–95, PW = 60–70), this ichnotaxon differs from *Occitanopodus* by low heteropody (1:2), asymmetric manual tracks with a large claw mark on the impression of digit I that is posteriorly oriented (Santos et al., 1994).

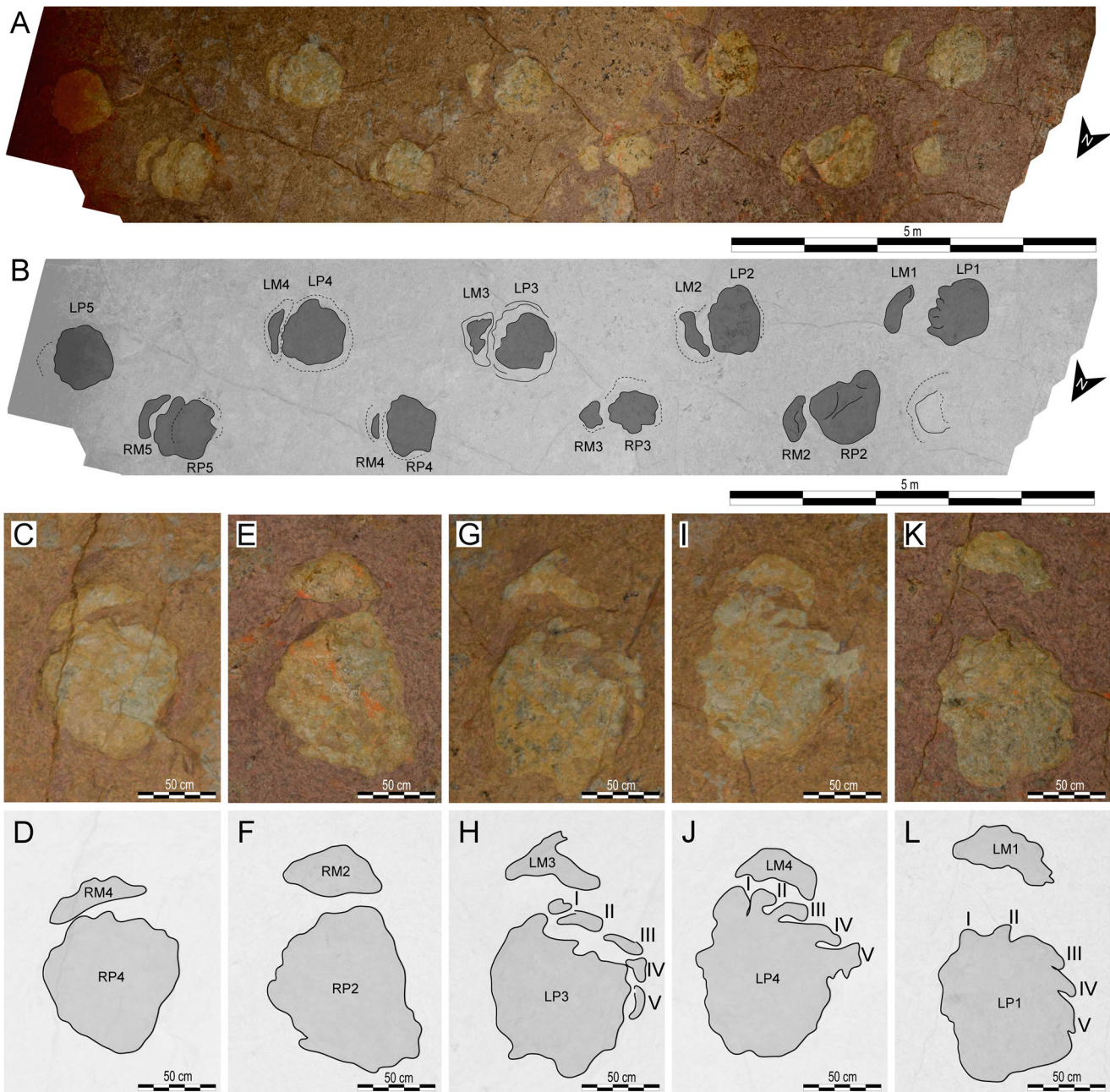


FIGURE 6. *Occitanopodus gandi*, igen. et isp. nov. A, photograph of trackway CAS-1; B, interpretive sketch. C–L, some pedal track–manual track sets of trackway CAS-1.

Excluding several ichnotaxa currently regarded as nomina dubia (Lockley et al., 1994; Wright, 2005), another ichnotaxon showing wide-gauge trackways was reported from the Upper Cretaceous of Argentina, *Titanopodus mendozensis* González Riga and Calvo, 2009. *Titanopodus mendozensis* differs from *Occitanopodus* by the outer limits of the trackway that are defined in some cases by manual prints, smaller tracks, lower heteropody (i.e., 1:3), and manual prints strongly rotated outward (i.e., 25–48°; González Riga and Calvo, 2009). The medium- to wide-gauge trackway *Oobardjidama foulkesi* was described from the Cretaceous deposits of Australia (Salisbury et al., 2017). *Oobardjidama foulkesi* mainly differs from *Occitanopodus* by a lower heteropody (30–45%), a smaller manual angulation (69–74°), and pedal

tracks with a lobed medial margin. Recently, Meyer et al. (2018) described *Calorckosauripus lazari* from Upper Cretaceous deposits of Bolivia. This wide/intermediate-gauge trackway with strong heteropody (1:1.85) differs from *Occitanopodus* by the smaller size of the tracks (PL = 49 cm and PW = 42 cm), lower values of PTR (22–34%), pedal tracks always longer than wide, and absence of digit impressions on pedal tracks.

Occitanopodus gandi, igen. et isp. nov. (trackway CAS-1), shows a unique combination of characters not observed amongst other Jurassic and Cretaceous sauropod tracks: wide-gauge trackway with pronounced heteropody up to 1:6; large-sized, as long as wide, pentadactyl, asymmetric, subcircular to oval pedal tracks with short digit impressions that show strong

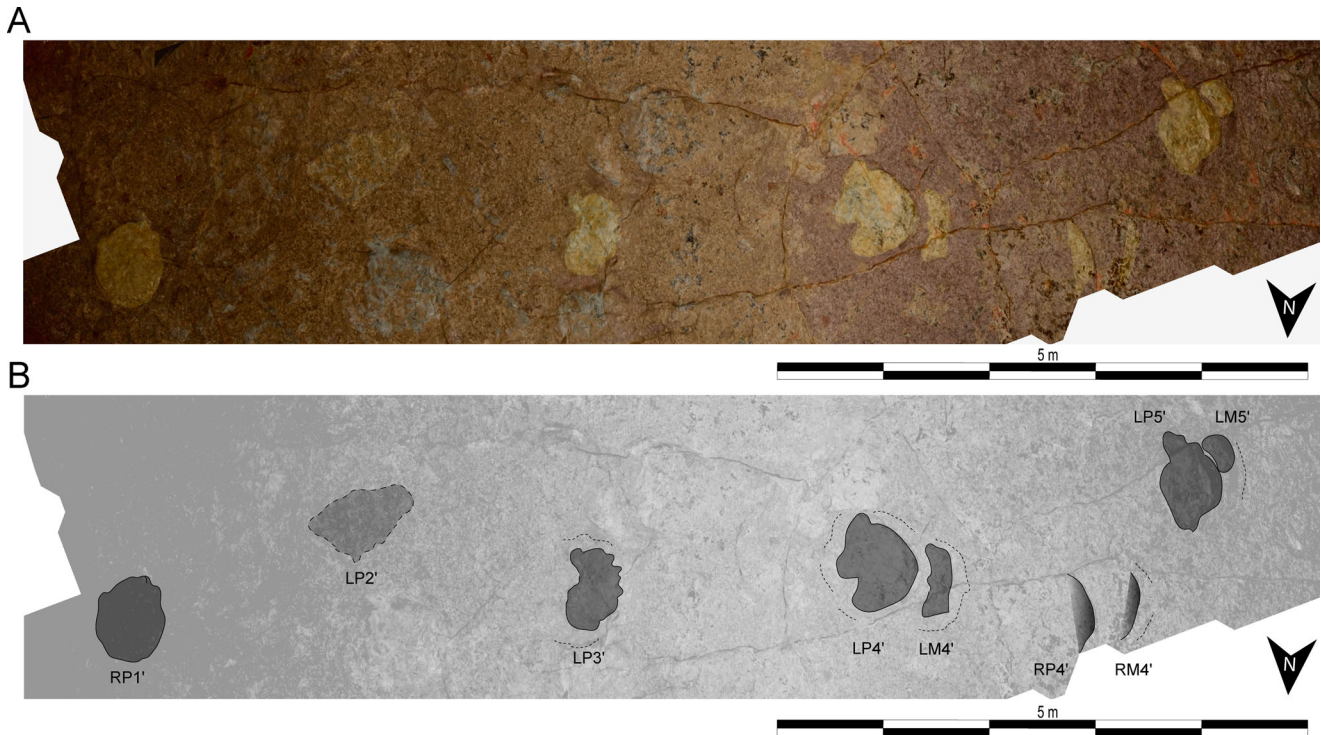


FIGURE 7. Trackway CAS-2. **A**, photogrammetric 3D textured mesh with texture; **B**, interpretive sketch.

outward rotation; symmetrical, ‘D’-shaped manual tracks lacking any indication of digits or claws; and pedal tracks and manual tracks forming a small positive rotation angle relative to the trackway axis.

Possible Trackmakers

The record of Middle Jurassic sauropod body fossils is very sparse worldwide (Weishampel et al., 2004). In Europe, sauropod skeletal remains from this epoch were mainly reported from the Aalenian–Callovian of England (e.g., Manning et al., 2015) and the Bathonian of Scotland (e.g., Clark et al., 1995; Barrett, 2006; Clark and Gavin, 2016). Bathonian–Callovian sediments from France only yield rare sauropod remains (Sauvage, 1900; Buffetaut, 1995; Buffetaut et al., 2011). Although the ‘Calcaires à stigmates’ Formation yielded some dinosaur teeth ascribed to ornithopods and theropods (Kriwet et al., 1997), sauropod body fossils are unknown in the Bathonian, as well as in any other Jurassic deposits from the Causses Basin. Some isolated bones and teeth ascribed to undetermined sauropods were reported from the Bathonian of the Indre Department and from the lower Callovian of Calvados, in northwestern France (Buffetaut, 1995). Only a lower Bathonian chevron bone from Les Ardennes Department was attributed to the eusauropod *Cetiosaurus* (Buffetaut et al., 2011). *Cetiosaurus* was reported from several Middle and Upper Jurassic localities in England (e.g., Owen, 1841; Benton and Spencer, 1995; Upchurch and Martin, 2003). According to Upchurch and Martin (2003), *Cetiosaurus* lies outside of, but is closely related to, the clade Neosauropoda.

The identity of the trackmakers of wide-gauge trackways has been debated for some time and is still problematic (Farlow, 1992; Wilson and Carrano, 1999). Many authors attributed wide-gauge trackways to brachiosaurids or titanosaurids (e.g., Wilson and Carrano, 1999; Day et al., 2002, 2004; Wilson, 2005), both included in the clade Titanosauriformes (Wilson

and Sereno, 1998; Wilson and Carrano, 1999). For example, according to Wilson (2005), the most common ichnotaxon showing wide-gauge trackways, *Brontopodus*, was likely made by a titanosauriform or possibly by saltasaurids, two clades originating in the Middle Jurassic and in the Early Cretaceous, respectively (Wilson, 2005). In contrast, Santos et al. (2009) proposed that wide-gauge trackways are not exclusive to Titanosauriformes and that *Polyonyx* was made by non-neosauropod eusauropods. Overall, it seems that the trackway gauge is not a reliable indicator of the trackmakers. Indeed, there are instances in which a single trackway changes from wide to narrow gauge (Leonardi and Avanzini, 1994; Wilson, 2005). Moreover, Lockley et al. (2002) suggested that titanosaurids may have changed from narrow gauge to wide gauge during growth. According to some authors (e.g., Marty et al., 2010; Meyer et al., 2018), gauge was probably influenced by behavior (different degrees of lateral bending, speed) or sexual dimorphism.

Manual tracks of *Occitanopodus* do not show any evidence of a large claw print on the impression of digit I (like tracks assigned to *Polyonyx*). It is not consistent with the predicted manual track morphology for diplodocoids and basal macronarians (Day et al., 2002; Wright, 2005). In contrast, titanosauriforms have reduced ungual phalanges on the manus (Day et al., 2004). The claw of digit I is reduced among brachiosaurids (i.e., *Brachiosaurus*), whereas it is missing among titanosaurids (Upchurch, 1994). Thus, despite some uncertainty, the best candidate for the trackmaker of *Occitanopodus* is a titanosauriform. The titanosauriforms are known from the Middle Jurassic to the Upper Cretaceous; they measured more than 30 m long, and the largest weighed more than 50 tons (Paul, 2010). In the absence of skeletal remains for this period in France, the tracks from Castelbouc may represent the first evidence of titanosauriforms in this area during the Middle Jurassic. This report complements the few other Middle Jurassic European tracksites yielding titanosauriform tracks (e.g., Day et al., 2002, 2004; Santos et al., 2009) and suggests that although the main

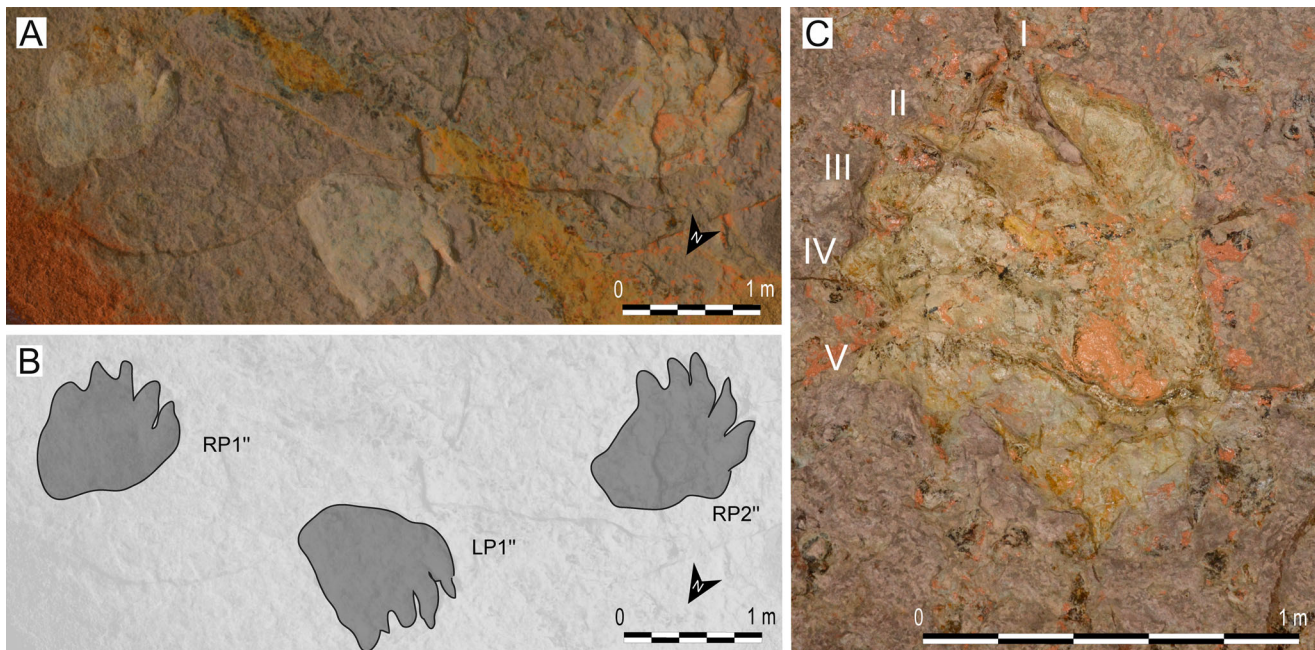


FIGURE 8. Trackway CAS-3. **A**, photogrammetric 3D textured mesh with texture; **B**, interpretive sketch. **C**, right foot of trackway CAS-3 (RP2'') showing traces of digits I–V.

radiation of the clade occurred during the Late Jurassic (Mannion et al., 2019), Titanosauriformes were probably present as early as the Middle Jurassic.

Paleoenvironmental Reconstruction

The presence of brachiopods, benthic foraminiferans, corals, and echinoids in the Castelbouc stratigraphic section attests that the depositional environments were in part marine. However, lignite beds yielding cuticles of conifers, wood, and terrigenous minerals (phyllosilicates, quartz, and rutile) indicate terrestrial inputs. In the context of the second main low sea level of the Tethys during the Jurassic filling of the Causses Basin, the co-occurrence of marine and terrestrial organisms suggests that the Castelbouc stratigraphic series was deposited in a panel of marginal-littoral paleoenvironments with possible brackish to euhaline conditions (Table 1). The surfaces bearing mud cracks and dinosaur trackways, as well as the main erosive surfaces, indicate that sediments were deposited in very proximal environments with a thin layer of water and which occasionally emerged.

Based on field observations associated with microfacies and mineralogical analyses, we identified various depositional environments (Table 1). They include (from the most proximal to the most distal) protected backshore areas not open to the sea (Facies F1); periodically emerged intertidal to supratidal zones (Facies F2); borders of bay or lagoon showing co-occurrence of strong marine and terrestrial inputs (possible brackish conditions) (Facies F5, F6); and foreshore (beach) to shoreface domains (Facies F3, F4, and F7).

Track preservation suggests that the ‘true’ walking surfaces are located in F6 and F7. The lignitic marly limestone of F6 suggests a shallow paralic environment commonly restricted but occasionally open to the sea, whereas F7 exhibits a strong marine influence. The depositional environment of F6 periodically emerged and recorded occasional hydrodynamic events, such as storms reworking material from the sea and transporting it into the paralic setting. The sauropods from Castelbouc walked along

beaches open to the sea and bays or lagoons sometimes affected by storms and floods that concentrated large amounts of plant remains locally. The occurrence of gypsum in Facies F6B suggests evaporitic conditions, but we cannot exclude that it is a newly formed karstic mineral.

Plant cuticles collected in the Tunnel gallery suggest the presence of a conifer-dominated forest along the coastline trampled by sauropods. All paleobotanical studies of the ‘Calcaires à Stipites’ Formation revealed plant macroremains, pollen, spores, and wood that attest diversified and abundant floras in freshwater to brackish littoral environments of the Causses Basin (Doubinger, 1961; Alabouvette et al., 1988; Philippe et al., 1998). Such vegetation was probably an attractive and important source of food for herbivorous dinosaurs. During the early to middle Bathonian, the regional climate was semiarid, changing to arid later in the Bathonian (Philippe et al., 1998).

Over the last few decades, bone microremains (Kriwet et al., 1997), as well as ichnological records (Sciau et al., 2006; Moreau et al., 2012; Moreau, 2017; Gand et al., 2018), suggested that Middle Jurassic environments from the Causses Basin were inhabited by dinosaur communities composed of ornithischians and theropods. The new tracks from Castelbouc attest the presence of giant sauropods in proximal littoral ecosystems, similar to what is observed in other Middle Jurassic tracksites (e.g., Castanera et al., 2014; Brusatte et al., 2015; dePolo et al., 2018). This discovery demonstrates the high potential for paleoichnological prospecting in deep karst caves that can sometimes offer larger and better-preserved rocky surfaces than outdoor outcrops.

CONCLUSIONS

The Bathonian sauropod tracks from the Castelbouc cave consist of three trackways: two quadrupedal, wide-gauge trackways and one pedal-track-only, narrow-gauge trackway. The new ichnotaxon *Occitanopodus gandi*, igen. et isp. nov. (trackway CAS-1), shows a combination of characters not observed amongst other Jurassic and Cretaceous sauropod tracks.

Stratigraphy, petrology, and mineralogy show that the sediments exposed in the Tunnel gallery were deposited in very proximal environments with a thin layer of water and which emerged occasionally. The tracksite from Castelbouc attests the presence of large sauropods such as Titanosauriformes in littoral environments during the Middle Jurassic. This report suggests that, although the main radiation of the clade occurred during the Late Jurassic, the Titanosauriformes were probably already present in Middle Jurassic ecosystems.

ACKNOWLEDGMENTS

We thank M. D'Emic, S. Salisbury, P. dePolo, and an anonymous reviewer for their constructive and thoughtful reviews on the manuscript. We thank G. Dumont and J. Dupont for technical assistance during photographic sessions. We express our gratitude to the Bouth family, owner of the entrance of the cave, who authorized the access to the cavity. We thank D. André, D. Bosc, and J.-C. Dufour for discussions and information about the cavity. We also thank J. Caboche and D. Betrancourt, from the Institut Mines Télécom (IMT) Lille Douai, for their contribution to mineralogical analyses. We express our gratitude to G. Gand who provided constructive comments on the manuscript. This publication is a contribution to the project 'Empreintes de dinosaures de la Grotte Castelbouc No. 4' led by the Association Paléontologique des Hauts Plateaux du Languedoc (Mende, Lozère, France).

LITERATURE CITED

- Ahlberg, A., and M. Siverson. 1991. Lower Jurassic dinosaur footprints in Helsingborg, southern Sweden. *Geologiska Föreningens i Stockholm Förhandlingar* 113:339–340.
- Alabouvette, B., J. P. Arondeau, M. Aubague, Y. Bodeur, P. Dubois, J. Mattei, H. Paloc, and J. P. Rançon. 1988. Notice explicative de la feuille Le Caylar à 1/50 000. Bureau de Recherches Géologiques et Minières, Orléans, France.
- Alexander, R. McN. 1976. Estimates of speeds of dinosaurs. *Nature* 261:129–130.
- André, D. 1992. Lozère des ténèbres. Spéléo Club de la Lozère, Saint-Georges-de-Luzençon, France, 257 pp.
- Barrett, P. M. 2006. A sauropod dinosaur tooth from the Middle Jurassic of Skye, Scotland. *Earth and Environmental Science Transactions of the Royal Society of Edinburgh* 97:25–29.
- Belvedere, M., P. Mietto, M. Avanzini, and M. Rigo. 2008. Norian dinosaur footprints from the "Strada delle Gallerie" (Monte Pasubio, NE Italy). *Studi Tridentini Scienze Naturali, Acta Geologica* 83:267–275.
- Benton, M. J., and P. S. Spencer. 1995. *Fossil Reptiles of Great Britain*. Chapman & Hall, London, 386 pp.
- Bish, D. L., and J. E. Post. 1993. Quantitative mineralogical analysis using the Rietveld full-pattern fitting method. *The American Mineralogist* 78:932–940.
- Brusatte, S. L., T. J. Challands, D. A. Ross, and M. Wilkinson. 2015. Sauropod dinosaur trackways in a Middle Jurassic lagoon on the Isle of Skye. *Scottish Journal of Geology* 52:1–9.
- Buffetaut, E. 1995. Un dinosaure saurope dans le Callovien du Calvados (Normandie, France). *Bulletin trimestriel de la Société géologique de Normandie et des amis du Muséum du Havre* 82:5–11.
- Buffetaut, E., B. Gibout, I. Launois, and C. Delacroix. 2011. The sauropod dinosaur *Cetiosaurus* Owen in the Bathonian (Middle Jurassic) of the Ardennes (NE France): insular, but not dwarf. *Carnets de Géologie* CG2011/06:149–161.
- Castanera, D., B. Vila, N. L. Razzolini, V. F. Santos, C. Pascual, and J. I. Canudo. 2014. Sauropod trackways of the Iberian Peninsula: palaeoecological and palaeoenvironmental implications. *Journal of Iberian Geology* 40:49–59.
- Charcosset, P. 2000. Synthèse paléogéographique et dynamique du bassin caussenard (Sud de la France) au cours du Bathonien (Jurassique moyen). *Eclogae Geologicae Helvetiae* 93:53–64.
- Charcosset, P., R. Ciszak, B. Peybernès, and J.-P. Garcia. 1996. Modalités séquentielles de la transgression bathonienne sur le 'Seuil cévenol' (Grands Causses). *Comptes Rendus Académie des Sciences de Paris* 323:419–426.
- Ciszak, R., B. Peybernès, J. Thierry, and P. Faure. 1999. Synthèse en termes de stratigraphie séquentielle du Dogger et de la base du Malm dans les Grands Causses. *Géologie de la France* 4:45–58.
- Clark, N. D., and P. Gavin. 2016. New Bathonian (Middle Jurassic) sauropod remains from the Valtos Formation, Isle of Skye, Scotland. *Scottish Journal of Geology* 52:71–75.
- Clark, N. D. L., J. D. Boyd, R. J. Dixon, and D. A. Ross. 1995. The first Middle Jurassic dinosaur from Scotland: a cetiosaurid? (Sauropoda) from the Bathonian of the Isle of Skye. *Scottish Journal of Geology* 31:171–176.
- Cignoni, P., M. Callieri, M. Corsini, M. Dellepiane, F. Ganovelli, and G. Ranzuglia. 2008. Meshlab: an open-source mesh processing tool; pp. 129–136 in V. Scarano, R. De Chiara, and U. Erra (eds.), *Eurographics Italian Chapter Conference*. Eurographics Association, Geneva, Switzerland.
- Cook, A. G., N. Saini, and S. A. Hocknull. 2010. Dinosaur footprints from the Lower Jurassic of Mount Morgan, Queensland. *Memoirs of the Queensland Museum* 55:135–146.
- Day, J. J., D. B. Norman, A. S. Gale, P. Upchurch, and H. P. Powell. 2004. A Middle Jurassic dinosaur trackway site from Oxfordshire, UK. *Paleontology* 47:319–348.
- Day, J. J., P. Upchurch, D. B. Norman, A. S. Gale, and H. P. Powell. 2002. Sauropod trackways, evolution, and behavior. *Science* 296:1659–1659.
- dePolo, P. E., S. L. Brusatte, T. J. Challands, D. Foffa, D. A. Ross, M. Wilkinson, and H.-Y. Yi. 2018. A sauropod dominated tracksite from Rubha nam Brathairean (Brothers' Point), Isle of Skye, Scotland. *Scottish Journal of Geology* 54:1–12.
- Doubinger, J. 1961. Spores et pollens des 'stipites' du Larzac (Bathonien). *Compte Rendu Sommaire des Séances de la Société Géologique de France*:162–163.
- Dutuit, J.-M., and A. Ouazzou. 1980. Découverte d'une piste de dinosaure saurope sur le site d'empreintes de Demnat (Haut Atlas marocain). *Mémoires de la Société géologique de France* 139:95–102.
- Ellenberger, P. 1988. La découverte des pistes de dinosauriens de Camprieu. *Causses et Cévennes* 7:139–140.
- Falkingham, P. L., K. T. Bates, L. Margetts, and P. L. Manning. 2011. Simulating sauropod manus-only trackway formation using finite-element analysis. *Biology Letters* 7:142–145.
- Farlow, J. O. 1992. Sauropod tracks and trackmakers: integrating the ichnological and skeletal records. *Zubia* 10:89–138.
- Farlow, J. O., J. G. Pittman, and J. M. Hawthorne. 1989. *Brontopodus birdi*, Lower Cretaceous sauropod footprints from the U.S. Gulf coastal plain; pp. 371–394 in D. D. Gillette and M. G. Lockley (eds.), *Dinosaur Tracks and Traces*. Cambridge University Press, Cambridge, U.K.
- Gand, G., G. Demathieu, and C. Montenat. 2007. Les traces de pas d'amphibiens, de Dinosaures et autres Reptiles du Mésozoïque français: inventaire et interprétations. *Palaeovertebrata* 35:1–149.
- Gand, G., E. Fara, C. Durlet, G. Caravaca, J.-D. Moreau, L. Baret, D. André, R. Lefillatre, A. Passet, M. Wiénin, and J.-P. Gély. 2018. Les pistes d'archosauroiens: *Kayentapus ubacensis* nov. sp. (théropodes) et crocodylomorphes du Bathonien des Grands-Causses (France). Conséquences paléo-biologiques, environnementales et géographiques. *Annales de Paléontologie* 104:183–216.
- González Riga, B. J., and J. O. Calvo. 2009. A new wide-gauge sauropod track site from the late Cretaceous of Mendoza, Neuquén Basin, Argentina. *Palaeontology* 52:631–640.
- Kim, J. Y., and M. G. Lockley. 2012. New sauropod tracks (*Brontopodus pentadactylus* ichnosp. nov.) from the Early Cretaceous Haman Formation of Jinju Area, Korea: implications for sauropods manus morphology. *Ichnos* 19:84–92.
- Kriwet, J., O. W. M. Rauhut, and U. Gloy. 1997. Microvertebrate remains (Pisces, Archosauria) from the Middle Jurassic (Bathonian) of southern France. *Neues Jahrbuch für Geologie und Paläontologie* 206:1–28.
- Le Loeuff, J., C. Gourrat, P. Landry, L. Hautier, R. Liard, C. Souillat, E. Buffetaut, and R. Enay. 2006. A Late Jurassic sauropod tracksite from southern Jura (France). *Comptes Rendus Palevol* 5:705–709.
- Leonardi, G., and M. Avanzini. 1994. *Dinosauri in Italia*. Le Scienze, Quadermi 76:69–81.
- Lockley, M. G., and A. P. Hunt. 1995. Ceratopsid tracks and associated ichnofauna from the Laramie Formation (Upper Cretaceous: Maastrichtian) of Colorado. *Journal of Vertebrate Paleontology* 15:592–614.

- Lockley, M. G., J. O. Farlow, and C. A. Meyer. 1994. *Brontopodus* and *Parabrontopodus* ichnogen. nov. and the significance of wide- and narrow-gauge sauropod trackways. *Gaia* 10:135–146.
- Lockley, M. G., A. S. Schulp, C. A. Meyer, G. Leonardi, and D. K. Mamani. 2002. Titanosaurid trackways from the Upper Cretaceous of Bolivia: evidence for large manus, wide-gauge locomotion and gregarious behaviour. *Cretaceous Research* 23:383–400.
- Manning, P. L., V. M. Egerton, and M. Romano. 2015. A new sauropod dinosaur from the Middle Jurassic of the United Kingdom. *PLoS ONE* 10:e0128107.
- Mannion, P. D., P. Upchurch, D. Schwarz, and O. Wings. 2019. Taxonomic affinities of the putative titanosaurs from the Late Jurassic Tendaguru Formation of Tanzania: phylogenetic and biogeographic implications for eusauropod dinosaur evolution. *Zoological Journal of the Linnean Society* 185:784–909.
- Marty, D. 2008. Sedimentology, taphonomy, and ichnology of Late Jurassic dinosaur tracks from the Jura carbonate platform (Chevenez-Combe Ronde tracksite, NW Switzerland): insights into the tidal-flat palaeoenvironment and dinosaur diversity, locomotion, and palaeoecology. *Geofocus* 21:1–278.
- Marty, D., M. Belvedere, C. A. Meyer, P. Mietto, G. Paratte, C. Lovis, and B. Thüring. 2010. Comparative analysis of Late Jurassic sauropod trackways from the Jura Mountains (NW Switzerland) and the central High Atlas Mountains (Morocco): implications for sauropod ichnotaxonomy. *Historical Biology* 22:109–133.
- Mazin, J.-M., P. Hantzpergue, and N. Olivier. 2017. The dinosaur tracksite of Plagne (early Tithonian, Late Jurassic; Jura Mountains, France): the longest known sauropod trackway. *Geobios* 50:279–301.
- Mazin, J.-M., P. Hantzpergue, and J. Pouech. 2016. The dinosaur tracksite of Loulle (early Kimmeridgian; Jura, France). *Geobios* 49:211–228.
- Meyer, C. A., D. Marty, and M. Belvedere. 2018. Titanosaur trackways from the Late Cretaceous El Molino Formation of Bolivia (Cal Orck'o, Sucre). *Annales Societatis Geologorum Poloniae* 88: 223–241.
- Milà, J. 2011. New theropod, thyreophoran, and small sauropod tracks from the Middle Jurassic Bagå Formation, Bornholm, Denmark. *Bulletin of the Geological Society of Denmark* 59:51–59.
- Milà, J., and R. G. Bromley. 2005. Dinosaur footprints from the Middle Jurassic Bagå Formation, Bornholm, Denmark. *Bulletin of the Geological Society of Denmark* 52:7–15.
- Moreau, J.-D. 2017. Des empreintes de dinosaures dans le Bathonien du Causses de Sauveterre. *Bulletin de la Société des Lettres, Sciences, et Arts de la Lozère* 44:75–81.
- Moreau, J.-D., L. Baret, G. Gand, E. Fara, C. Durlet, and G. Caravaca. 2012. Découverte d'un nouveau site à traces de pas de Dinosaures dans le Bathonien des Causses (Le Gayrand, Gorges de la Jonte, Lozère, France); pp. 13–19 in *Ichnologie dinosaureenne du Jurassique de Meyrueis*. Association Paléontologique des Hauts Plateaux du Languedoc, Mende, France.
- Moreau, J. D., V. Trincal, D. André, L. Baret, A. Jacquet, and M. Wienin. 2018. Underground dinosaur tracksite inside a karst of southern France: Early Jurassic tridactyl traces from the Dolomitic Formation of the Malaval Cave (Lozère). *International Journal of Speleology* 47:29–42.
- Owen, R. 1841. A description of a portion of the skeleton of *Cetiosaurus*, a gigantic extinct saurian occurring in the Oolitic Formation of different parts of England. *Proceedings of the Geological Society of London* 3:457–462.
- Parker, L. R., and J. K. Balsley. 1989. Coal mines as localities for studying dinosaur trace fossils; pp. 353–359 in D. D. Gillette and M. G. Lockley (eds.), *Dinosaur Tracks and Traces*. Cambridge University Press, Cambridge, U.K.
- Paul, G. S. 2010. *The Princeton Field Guide to Dinosaurs*. Princeton University Press, Princeton, New Jersey, 177 pp.
- Peterson, W. 1924. Dinosaur tracks in the roofs of coal mines. *Natural History* 24:388–397.
- Philippe, M., F. Thévenard, G. Barale, G. Guignard, and S. Ferry. 1998. Middle Bathonian floras and phytocoenoses of France. *Palaeogeography, Palaeoclimatology, Palaeoecology* 143:135–158.
- Romano, M., M. A. Whyte, and P. L. Manning. 1999. New sauropod dinosaur prints from the Saltwick Formation (Middle Jurassic) of the Cleveland Basin, Yorkshire. *Proceedings of the Yorkshire Geological and Polytechnic Society* 52:361–369.
- Rouire, L. 1946. Lignites du Larzac. Deuxième partie. Mines et Concessions 26:317–367.
- Salisbury, S. W., A. Romilio, M. C. Herne, R. T. Tucker, and J. P. Nair. 2017. The dinosaurian ichnofauna of the Lower Cretaceous (Valanginian-Barremian) Broome Sandstone of the Walmadany Area (James Price Point), Dampier Peninsula, Western Australia. *Society of Vertebrate Paleontology Memoir* 16. *Journal of Vertebrate Paleontology* 36(1, Supplement):1–152.
- Santos, V. F., J. J. Moratalla, and R. Royo-Torres. 2009. New sauropod trackways from the Middle Jurassic of Portugal. *Acta Palaeontologica Polonica* 54:409–422.
- Santos, V. F., M. G. Lockley, C. A. Meyer, J. Carvalho, A. M. Galopim de Carvalho, and J. J. Moratalla. 1994. A new sauropod tracksite from the Middle Jurassic of Portugal. *Gaia* 10:5–13.
- Sauvage, H.-E. 1900. Note sur les poissons et les reptiles du Jurassique inférieur du département de l'Indre. *Bulletin de la Société Géologique de France* 28:500–504.
- Schneider, C. A., W. S. Rasband, and K. W. Eliceiri. 2012. NIH Image to ImageJ: 25 years of image analysis. *Nature Methods* 9:671–675.
- Sciau, J., M. Bécaud, and G. Gand. 2006. Présence de Dinosaures Théropodes et probablement d'Ornithopodes et de Sauropodes dans le marais maritime Bajocien-Bathonien des Causses. *Association des Amis du Musée de Millau*, Millau, France, 32 pp.
- Taylor, J. C., and I. Hinczak. 2003. *Rietveld made easy: a practical guide to the understanding of the method and successful phase quantifications*. Sietronics Pty. Ltd., Canberra, Australia.
- Thulborn, T. 1990. *Dinosaur Tracks*. Chapman & Hall, London, 410 pp.
- Trincal, V., V. Thiéry, Y. Mamindy-Pajany, and S. Hillier. 2018. Use of hydraulic binders for reducing sulphate leaching: application to gypsiferous soil sampled in Ile-de-France region (France). *Environmental Science and Pollution Research International* 25:22977–22997.
- Trincal, V., D. Charpentier, M. D. Bautier, B. Grobety, B. Lacroix, B. P. Labaume, and J.-P. Sizun. 2014. Quantification of mass transfers and mineralogical transformations in a thrust fault (Monte Perdido thrust unit, southern Pyrenees, Spain). *Marine and Petroleum Geology* 55:160–175.
- Upchurch, P. 1994. Manus claw function in sauropod dinosaurs. *Gaia* 10:161–171.
- Upchurch, P., and J. Martin. 2003. The anatomy and taxonomy of *Cetiosaurus* (Saurischia, Sauropoda) from the Middle Jurassic of England. *Journal of Vertebrate Paleontology* 23:208–231.
- Weishampel, D. B., P. Dodson, and H. Osmólska. 2004. *The Dinosauria*. University of California Press, Berkeley, California, 733 pp.
- Wilson, J. A. 2005. Integrating ichnofossil and body fossil records to estimate locomotor posture and spatiotemporal distribution of early sauropod dinosaurs: a stratocladistic approach. *Paleobiology* 31:400–423.
- Wilson, J. A., and M. T. Carrano. 1999. Titanosaurs and the origin of “wide-gauge” trackways: a biomechanical and systematic perspective on sauropod locomotion. *Paleobiology* 25:252–267.
- Wilson, J. A., and P. Sereno. 1998. Early evolution and higher level phylogeny of sauropod dinosaurs. *Society of Vertebrate Paleontology Memoir* 5. *Journal of Vertebrate Paleontology* 18(2, Supplement):1–68.
- Wright, J. L. 2005. Steps in understanding sauropod biology—the importance of sauropod tracks; pp. 252–280 in K. A. Curry Rogers and J. A. Wilson (eds.), *The Sauropods: Evolution and Paleobiology*. University of California Press, Berkeley, California.

Submitted October 29, 2018; revisions received December 4, 2019; accepted December 13, 2019.

Handling editor: Michael D'Emic